International Journal of Theoretical Physics, Vol. 33, No. 2, 1994

Dispersion, Topological Scattering, and Self-Interference in Multiply Connected Robertson–Walker Cosmologies

Roman Tomaschitz[1]

Received March 2, 1993

We investigate scattering effects in open Robertson–Walker cosmologies whose spacelike slices are multiply connected hyperbolic manifolds. We work out an example in which the 3-space is infinite and has the topology of a solid torus. The world-lines in these cosmologies are unstable, and classical probability densities evolving under the horospherical geodesic flow show dispersion, as do the densities of scalar wave packets. The rate of dispersion depends crucially on the expansion factor, and we calculate the time evolution of their widths. We find that the cosmic expansion can confine dispersion: The diameter of the domain of chaoticity in the 3-manifold provides the natural, time-dependent length unit in an infinite, multiply connected universe. In a toroidal 3-space manifold this diameter is just the length of the limit cycle. On this scale we find that the densities take a finite limit width in the late stage of the expansion. In the early stage classical densities and conformally coupled fields approach likewise a finite width; nonconformally coupled fields disperse. Self-interference occurs if the dispersion on the above scale is sufficiently large, so that the wave packet can overlap with itself. Signals can be backscattered through the topology of 3-space, and we calculate their recurrence times.

1. INTRODUCTION

In this paper we deal with the topological structure of space-time, in particular with the bearing of the topology on the microscopic motion, on the global behavior of the world-lines, and on the dynamics of wave packets.

We assume that the metric tensor of space-time can locally be described by a Robertson–Walker (RW) line element, and that the 3-space is infinite and has negative curvature.

[1]Theoretical Physics Group, Tata Institute of Fundamental Research, Bombay 400 005, India, and Physics Department, University of the Witwatersrand, Johannesburg, WITS 2050, South Africa.

0020-7748/94/0200-0353$07.00/0

In Tomaschitz (1993*a*) we compared in the simply connected topology of the Minkowski hyperboloid the dispersion of classical densities that arises because of the instability of the flow lines with the dispersion of quantum mechanical wave packets. We found asymptotic equivalence of the classical and quantum dispersion in regimes where no annihilation/production processes occur. This is an important result, because it shows that in these universes the classical instability is well capable of producing the same dispersion phenomena as wave fields.

As was pointed out at length in the preceding papers (Tomaschitz, 1992*a*–*c*), a further peculiarity of open RW cosmologies of negative spatial curvature is that the spacelike slices can take a variety of topologies, which can even change in time.

If the 3-space is multiply connected and infinite, it is metrically deformable; its metric can vary in time even if its Gaussian curvature stays constant, in sharp contrast to the rigidity of the simply connected RW cosmologies with S^3, $\mathbb{R}^3$, H^3 as spacelike slices.

Another striking topological effect is the appearance of regions of chaoticity, and of bound-state wave fields localized on them (Tomaschitz, 1991).

In this paper we study topological scattering phenomena arising because of the multiple connectivity of the 3-space. Properly speaking, if a signal is emitted at some time, then a fraction of it may come back at later instants from different directions. This backscattering is somewhat reminiscent of the scattering that wave packets undergo in a metric that is rapidly varying in time (Schrödinger, 1939, 1956).

In Section 2 we study horospherical geodesic flows in a multiply connected 3-space manifold. Such a flow consists of bundles of parallel geodesics issuing from the boundary at infinity of the 3-space. We study probability densities evolving under this flow, and we derive a continuity equation for the 4-current density.

In Section 3 we compare this current with the current of wave fields satisfying the Klein–Gordon equation. In the case of the Minkowski hyperboloid as 3-space we found (Tomaschitz, 1993*a*) asymptotic equivalence of the classical current and the quantum current in regimes where we can identify positive- and negative-frequency solutions, for example, when the expansion factor is slowly varying. If the 3-space is multiply connected, this equivalence can be destroyed by topological scattering and the arising self-interference of the wave packet.

In Section 4 we make some comments on the topologies we have in mind, and sketch the simplest example of a hyperbolic 3-manifold that is open and multiply connected, namely that of a solid torus.

In Section 5 we study topological scattering in RW cosmologies whose spacelike slices are solid tori. We will here again recognize the central part that the convex hull of the limit set of the covering group plays (Tomaschitz, 1992*a*). Its projection into the torus gives the limit cycle, a closed loop from which particles are spiraling out in infinite cycles. We study the scattering and dispersion of horospherical flows in the early and late stages of the expansion; in the quantum case we study self-interference. The expansion of 3-space provides a mechanism to confine dispersion. In fact, if we measure the widths of the densities in units of the circumference of the expanding limit cycle, we have the surprising phenomenon that wave packets as well as classical densities have finite limit widths. For further discussion on that we refer to the conclusion, Section 6.

2. HOROSPHERICAL FLOWS IN RW COSMOLOGIES: THE GENERAL SETTING

In Tomaschitz (1993*a*) we introduced the concept of a horospherical flow in a simply connected RW cosmology of negative spatial curvature, i.e., with Minkowski hyperboloids as spacelike slices. We constructed a 4-current j_c^μ, a continuity equation, and an invariant measure. The full power of horospherical flows appears in the context of RW cosmologies whose spacelike slices are multiply connected hyperbolic 3-manifolds.

We formulate in this paper the concept of a horospherical flow on a multiply connected space-time manifold with the line element

$$ds^2 = -c^2\,d\tau^2 + a^2(\tau)\,d\sigma^2 \tag{2.1}$$

Here $d\sigma^2$ denotes the line element of the open 3-space manifold, which we represent as a fundamental polyhedron F in the Poincaré ball B^3, or in the half-space model H^3 of hyperbolic space. The discrete group generated by the identifying transformations of the polyhedral faces we denote by Γ. For more details we refer to Tomaschitz (1992*a*).

We start with the continuity equation in $\mathbb{R}^{(+)} \times B^3$, which projects as it stands onto the manifold $\mathbb{R}^{(+)} \times F$, because of the invariance of $d\sigma^2$ under the Lorentz group, of which Γ is a discrete subgroup:

$$\frac{1}{\sqrt{-g}}\frac{\partial}{\partial x^\mu}(\sqrt{-g}\,j^\mu) = 0 \tag{2.2}$$

Similar to the wave equation, we get solutions of (2.2) on the manifold $\mathbb{R}^{(+)} \times F$ by periodizing (method of images) with the covering group Γ a solution $j^\mu_{B^3}$ in B^3. In fact we get all solutions in this way.

Let $x^\mu = (\tau, \mathbf{x})$, $\mathbf{x} \in B^3$, and $\gamma \in SO^+(3, 1)$, the invariance group of B^3. We consider coordinate transformations of the kind $\tau' = \tau$, $\mathbf{x}' = \gamma^{-1}\mathbf{x}$,

leaving $g_{\mu\nu}$, the metric tensor of (2.1), invariant. The Jacobian $\partial x'^{\nu}/\partial x^{\mu}$ we denote by $[\gamma^{-1'}x]^{\nu}_{\mu}$; restricted to 3-space it is just the $\gamma^{-1'}\mathbf{x}$ explicitly given in Tomaschitz (1993*a*).

Clearly we have the following transformation rules (Landau and Lifshitz, 1971):

$$j_{\mu}(x) = [\gamma^{-1'}x]^{\nu}_{\mu} j'_{\nu}(x'), \qquad [\gamma' x']^{-1\mu}_{\nu} = [\gamma^{-1'}x]^{\mu}_{\nu} \tag{2.3}$$

$$[\gamma' x']^{\lambda}_{\mu} g^{\mu\nu}(x') = [\gamma^{-1'}x]^{\nu}_{\mu} g^{\mu\lambda}(x) \tag{2.4}$$

$$\frac{1}{[-g(x)]^{1/2}} \frac{\partial}{\partial x^{\mu}} \{[-g(x)]^{1/2} j^{\mu}(x)\}$$

$$= \frac{1}{[-g(x')]^{1/2}} \frac{\partial}{\partial x'^{\mu}} \{[-g(x')]^{1/2} [\gamma' x']^{-1\mu}_{\nu} j^{\nu}(\gamma x')\} \tag{2.5}$$

We define formally the Poincaré series

$$j^{\mu}_{\Gamma}(x) = (\rho_{\Gamma}, \mathbf{j}_{\Gamma}) := \sum_{\gamma \in \Gamma} [\gamma' x]^{-1\mu}_{\nu} j^{\nu}(\gamma x) \tag{2.6}$$

$$\rho_{\Gamma}(\mathbf{x}, \tau) = \sum_{\gamma \in \Gamma} \rho(\gamma \mathbf{x}), \qquad \mathbf{j}_{\Gamma}(\mathbf{x}, \tau) = \sum_{\gamma \in \Gamma} [\gamma' x]^{-1} \mathbf{j}(\gamma \mathbf{x}) \tag{2.7}$$

$[\gamma' \mathbf{x}]$ is the Jacobian of γ in B^3.

Using the chain rule for Jacobians, we have for $g \in \Gamma$

$$\rho_{\Gamma}(g\mathbf{x}) = \rho_{\Gamma}(\mathbf{x}), \qquad \mathbf{j}_{\Gamma}(g\mathbf{x}) = [g'\mathbf{x}]\, \mathbf{j}_{\Gamma}(\mathbf{x}) \tag{2.8}$$

Applying (2.5), we see that j^{μ}_{Γ} satisfies (2.2) provided j^{μ} does. (j^{μ}_{Γ} must be absolutely convergent, since there is no natural order of the elements in Γ.)

The standard way to estimate the convergence of Poincaré series in B^3 is to reduce them to series of the type

$$\sum_{\gamma \in \Gamma} (1 - |\gamma \mathbf{x}|^2)^{\lambda}, \qquad \lambda \in \mathbb{C} \tag{2.9}$$

and the convergence behavior of such series is well known (Patterson, 1987; Mandouvalos, 1988). The abscissa of convergence is the Hausdorff dimension δ of the limit set $\Lambda(\Gamma)$ of Γ, $0 \le \delta < 2$, i.e., (2.9) converges for $\mathrm{Re}(\lambda) > \delta$.

In Tomaschitz (1993*a*) we constructed Gaussian densities evolving under a flow of parallel geodesics in B^3 issuing from a point η at infinity of hyperbolic space. The surfaces of constant action are horospheres, namely spheres that meet S_{∞} (the boundary of B^3) tangentially at η.

We obtained for the time evolution of a classical density under this flow

$$\rho_c(\mathbf{x}, \tau, \eta) \sim \frac{a^{-3}(\tau) P^2(\mathbf{x}, \eta)}{[1 + 2\alpha^2\beta^2 B^2(\tau)]^{1/2}} \exp\left[\frac{-\alpha^2(\log P(\mathbf{x}, \eta) + A(\tau))^2}{1 + 2\alpha^2\beta^2 B^2(\tau)}\right] \tag{2.10}$$

Here β refers to the energy averaging, α to the spatial width of the initial packet, P is the Poisson kernel, $P(\mathbf{x}, \eta) = (1 - |\mathbf{x}|^2)/|\mathbf{x} - \eta|^2$, $\eta \in S_\infty$, and

$$A(\tau) = \frac{c}{R} \int_{\tau_0}^{\tau} a^{-1}(\tau)[1 + v_0^{-2} c^{-2} a^2(\tau)]^{-1/2} \, d\tau, \qquad B(\tau) = \frac{\partial A}{\partial v_0} \tag{2.11}$$

where R is the radius of B^3 (Gaussian curvature $-1/R^2$); v_0 is connected with the expectation value of the energy via $E_0 = mc^2[1 + c^2 v_0^2 a^{-2}(\tau)]^{1/2}$.

With (2.10) we construct the first series in (2.7). We assume at first that η is not in the limit set $\Lambda(\Gamma)$, which is a set of Lebesgue measure zero on S_∞. Then the denominator $|\gamma \mathbf{x} - \eta|$ of P is uniformly bounded from below for fixed $\mathbf{x}, \eta$, and we can estimate

$$\rho_\Gamma < \text{const} \cdot \sum_\gamma \tilde{P}(\gamma \mathbf{x})^{2 - \lambda \log \tilde{P}(\gamma \mathbf{x})[1 + A/\log \tilde{P}(\gamma \mathbf{x})]^2} \tag{2.12}$$

with $\lambda = \alpha^2/(1 + 2\alpha^2\beta^2 B^2)$, where we have replaced P in (2.10) by $\tilde{P}(\mathbf{x}) = \text{const} \cdot (1 - |\mathbf{x}|^2)$. Comparing (2.12) with (2.9), we see that the convergence is excellent, since the exponent converges to infinity.

In fact, because of the exponential in (2.10) the series ρ_Γ even converges if η is in the limit set. To see that, we note that because $|\eta| = 1$ we have $(1 - |\mathbf{x}|)/2 < P < 2/(1 - |\mathbf{x}|)$ if $|\mathbf{x}|$ is close to one. The replacement $\tilde{P} \to 1/\tilde{P}$ in (2.12) gives again an exponent convergent to $+\infty$.

The series for $\mathbf{j}_\Gamma$ in (2.7) we can estimate on the same footing; for the Jacobi determinant $|\gamma' \mathbf{x}|^3$ we use the formula $|\gamma' \mathbf{x}| = (1 - |\gamma \mathbf{x}|^2)/(1 - |\mathbf{x}|^2)$ and for the logarithmic derivative of the Poisson kernel that appears in the particle velocity ($\mathbf{j} = \mathbf{v}\rho$) we use $|\partial \log P/\partial \mathbf{x}| = 2/(1 - |\mathbf{x}|^2)$.

3. HOW TO TRACE THE CLASSICAL CURRENT IN THE QUANTUM CURRENT

The scalar wave equation

$$\frac{1}{\sqrt{-g}} \frac{\partial}{\partial x^\mu} \left(\sqrt{-g}\, g^{\mu\nu} \frac{\partial}{\partial x^\nu} \psi \right) - \left(\frac{mc}{\hbar} \right)^2 \psi - \xi \hat{R} \psi = 0 \tag{3.1}$$

in a multiply connected RW cosmology has been discussed in Tomaschitz (1991, 1992*b*). We use the same notation and sign conventions. ξ is the coupling to the curvature scalar $\hat{R}$ of (2.1).

Due to the invariance of $g_{\mu\nu}$ under $\mathbf{x}' = \gamma^{-1}\mathbf{x}$ [cf. Eq. (2.4)] we obtain

$$\psi^\Gamma(x) = \sum_{\gamma \in \Gamma} \psi(\gamma \mathbf{x}) \tag{3.2}$$

as a solution of (3.1) on the manifold $\mathbb{R}^{(+)} \times F$, provided ψ solves (3.1). We assume as in Section 2 the absolute convergence of (3.2); see below.

The quantum current $j_q^{\Gamma\mu}$ on the 4-manifold we define as usual via

$$j_q^{\Gamma\mu} = \frac{c^2}{2i} g^{\mu\nu}\left[\overline{\psi^\Gamma}\frac{\partial}{\partial x^\nu}\psi^\Gamma - \psi^\Gamma \frac{\partial}{\partial x^\nu}\overline{\psi^\Gamma}\right] \tag{3.3}$$

It satisfies the continuity equation (2.2) because ψ^Γ solves (3.1).

In order to extract the classical current from $j_q^{\Gamma\mu}$, we write (3.3) as

$$j_q^{\Gamma\mu} = \sum_{(\alpha,\beta)\in\Gamma\times\Gamma} j^\mu_{\alpha\beta} \tag{3.4}$$

with

$$j^\mu_{\alpha\beta} = \frac{c^2}{4i} g^{\mu\nu}(x)\left[\overline{\psi(\alpha x)}\frac{\partial}{\partial x^\nu}\psi(\beta x) + (\alpha \leftrightarrow \beta) - c.c.\right] \tag{3.5}$$

Applying the wave equation, we see immediately that also the image currents $j^\mu_{\alpha\beta}$ in B^3 are conserved,

$$\frac{1}{\sqrt{-g}}\frac{\partial}{\partial x^\mu}(\sqrt{-g}\, j^\mu_{\alpha\beta}) = 0 \tag{3.6}$$

The reordering of terms in moving from (3.3) to (3.4) is allowed because of the absolute convergence of (3.2). Because $j_q^{\Gamma\mu}$ in (3.4) remains unchanged if we replace $j^\mu_{\alpha,\beta}$ by $j^\mu_{\alpha g,\beta g}$, $g\in\Gamma$, and because of the invariance of $g_{\mu\nu}$, one finds again (2.8) satisfied with the $j_q^{\Gamma\mu}$ of (3.3).

In Tomaschitz (1993*a*) we constructed Gaussian wave packets by averaging over a complete set of solutions of (3.1),

$$\psi = \frac{1}{(2\pi)^{1/2}\alpha}\int_{-\infty}^{+\infty} ds\, \varphi(\tau, s) P^{1-is}(\mathbf{x}, \eta)\exp\frac{(s-s_0)^2}{2\alpha^2} \tag{3.7}$$

and by steepest descent,

$$\psi \sim \frac{1}{(1+i\alpha^2 f_{,ss})^{1/2}}\varphi(\tau, s_0)P^{1-is_0}(\mathbf{x}, \eta)\exp\left[\frac{-\alpha^2}{2}\frac{(\log P + f_{,s})^2}{1+i\alpha^2 f_{,ss}}\right] \tag{3.8}$$

s denotes the spectral variable, and $\varphi = Ae^{-if}$ is a positive frequency solution. We assume here that we are in a regime where we can disentangle positive and negative frequencies; see the examples (5.13)–(5.15) and Tomaschitz (1992*c*, 1993*a*). To obtain the wave field on the manifold $\mathbb{R}^{(+)} \times F$, we periodize (3.7). We can do this by inserting the asymptotic expression (3.8) into equation (3.2), or by periodizing ψ in (3.7) under the integral sign, writing

$$\psi^\Gamma = \frac{1}{(2\pi)^{1/2}\alpha}\int_{-\infty}^{+\infty} ds\, \varphi(\tau, s) E(\mathbf{x}, \eta, 1-is)\exp\frac{(s-s_0)^2}{2\alpha^2} \tag{3.9}$$

with the Eisenstein series (Mandouvalos, 1988)

$$E(\mathbf{x}, \eta, \alpha) = \sum_{\gamma \in \Gamma} P^{\alpha}(\gamma \mathbf{x}, \eta) \tag{3.10}$$

which constitute if $\alpha = 1 - is$, $s \in \mathbb{R}$, the generalized eigenfunctions of the Laplace–Beltrami operator Δ on the spacelike sections,

$$-\Delta E(\mathbf{x}, \eta, 1 - is) = (1 + s^2) E(\mathbf{x}, \eta, 1 - is) \tag{3.11}$$

η is a degeneration index, ranging on the free faces of F on S_{∞}.

The convergence abscissa of (3.10) is just the Hausdorff dimension δ of $\Lambda(\Gamma)$; see (2.9). For $\mathrm{Re}(\alpha) > \delta$ the series in (3.10) converges well, but not fast enough to get really accurate results; see, e.g., the determination of the abscissa of convergence in Tomaschitz (1992*a*). If $\delta > 1$, i.e., if there is a bound state, $E(\mathbf{x}, \eta, 1 - is)$ is still determined by the analytic continuation of the series (3.10), but it cannot be constructed explicitly. Therefore it is in practice by far preferable to avoid the spectral resolution of Δ on F, and to project B^3-wave packets into F by periodizing them via equation (3.2). The series in (3.2) is analogous to (2.7), (2.12) and is rapidly convergent because of the exponential in (3.8).

We denote the current of a solution ψ of (3.1) in B^3 by j_q^{μ}, i.e., j_q^{μ} is given by (3.3) with ψ^{Γ} replaced by ψ. With the ψ of (3.8) we have

$$j_q^0 = \rho_q \sim \frac{a^{-3}(\tau) P^2}{(1 + \alpha^4 f_{,ss}^2)^{1/2}} \exp\left[\frac{-\alpha^2 (\log P + f_{,s})^2}{1 + \alpha^4 f_{,ss}^2}\right] \tag{3.12}$$

It follows easily from the definition of $j_{\alpha\beta}^{\mu}$ in (3.5) that

$$\mathrm{diag}(j_q^{\Gamma\mu}) := \sum_{(\gamma,\gamma) \in \Gamma \times \Gamma} j_{\gamma\gamma}^{\mu}(x) = \sum_{\gamma \in \Gamma} [\gamma' x]^{-1}{}_{\nu}^{\mu} j_q^{\nu}(\gamma x) \tag{3.13}$$

In Tomaschitz (1993*a*) it has been shown that in the case of the adiabatic variation of the expansion factor $a(\tau)$, in the late stage of the expansion, and, if the wave field is conformally coupled, also at the beginning of the expansion, we have

$$j_c^{\mu}(x) \sim j_q^{\mu}(x) \tag{3.14}$$

($\sim$: time asymptotics). From (3.13), (3.14), and (2.6) it follows that the diagonal part of the quantum current is asymptotically equivalent to the classical 4-current,

$$\mathrm{diag}(j_q^{\Gamma\mu}) \sim j_c^{\Gamma\mu} \tag{3.15}$$

A wave packet in the simply connected topology of the Minkowski hyperboloid B^3 cannot interfere with itself, and (3.14) expresses the equivalence of the classical and quantum dispersion.

However, if the 3-space is multiply connected, as in the examples of the next two sections, one has topological scattering, and the scattered wave trains interfere. This interference is accounted for in the off-diagonal elements of $j^{\mu}_{\alpha\beta}$ in (3.5), which make the difference from the classical current. For further discussion we refer to Section 5.

4. THE TOPOLOGY OF THREE-SPACE

Before we discuss the preceding more explicitly for infinite RW cosmologies whose space-like sections are solid tori, we make some comments on the possible topologies of the spacelike slices and the discrete groups associated with them. Positively and zero-curved 3-manifolds are very exceptional, likewise negatively curved (=hyperbolic) 3-manifolds of finite volume. There exist two generic classes of open hyperbolic manifolds, which are topologically either hollow or solid handle bodies. The first are the product of a sphere with some (at least two) handles attached and a finite open interval (thickened Riemann surfaces). The second are the product of an open disk with some (at least one) closed disks cut out and a finite open interval.

A solid handle body may be realized in H^3 as follows (Krushkal *et al.*, 1986). We choose $2n$ mutually disjoint closed disks in the complex plane and identify their boundary circles in pairs with hyperbolic or loxodromic Möbius transformations, so that the interior of one circle is mapped onto the exterior of the second.

Now we regard the complex plane as the boundary of the hyperbolic half-space H^3, place hemispheres on the circles, and lift (e.g., Beardon, 1983) the Möbius transformations to H^3. The fundamental polyhedron of the handle body is then the space above the hemispheres, the polyhedral faces are these hemispheres that are identified in pairs by the lifted transformations, and there is also one free face, namely the complex plane with the $2n$ disks removed, which is the boundary surface of the handle body, where the hyperbolic metric gets singular. That this polyhedron is topologically a solid handle body of genus n is best seen in the B^3 model; the hemispheres then get spherical caps on S_∞. Pulling them out into the exterior of B^3 and gluing them together in pairs, we obtain the topological handle body. The covering group Γ generated by the face-identifying transformations gives, if applied to this polyhedron, a tessellation of H^3 whose accumulation points constitute the limit set (Akaza, 1964).

The simplest example of an open, topologically nontrivial hyperbolic manifold is, as mentioned, a solid torus. Its covering group is cyclic; the limit set consists of two points (Ford, 1951): We choose two disjoint disks ($n = 1$) in the complex plane, and identify their boundaries with a hyper-

bolic or loxodromic Möbius transformation T that maps the interior of the one onto the exterior of the other. The fundamental polyhedron is then obtained by placing hemispheres onto the two circles. An isometric copy F of this polyhedron we obtain if we conjugate T so that its fixed points are 0 and ∞. The conjugated transformation is $z \to Kz$ (K is the modulus of T, w.l.o.g. $|K| > 1$, otherwise we take T^{-1}). This transformation can be lifted to H^3 as T_K: $(z, t) \to (Kz, |K|t)$. A fundamental polyhedron F for the cyclic covering group Γ_K: $(z, t) \to (K^n z, |K|^n t)$, $n \in \mathbb{Z}$, generated by T_K, is the space between the two concentric hemispheres on the base circles $|z| = 1$ and $|z| = |K|$ above the annulus defined by these two circles; see Fig. 1. The two fixed points 0 and ∞ of T_K are the limit points of Γ_K: Applying Γ_K to F, we get a tiling $\Gamma_K(F)$ of H^3 with accumulation points 0 and ∞.

Though the geodesics on a solid torus are unstable and may have very complicated shapes, they are never chaotic, even not ergodic, and there do not exist bound states and localized wave fields, contrary to the hollow handle bodies with quasi-Fuchsian covering groups discussed in Tomaschitz (1991). The continuous spectrum of the wave equation remains the same as in the topologically trivial case with the Minkowski hyperboloid as 3-space (Mandouvalos, 1988). The qualitative behavior of geodesics on the manifold can be studied easily, in particular their topology, likewise horospherical flows and the topology of horospherical wavefronts. Moreover, the Poincaré series defining the currents introduced in Sections 2 and 3 reduce to Jacobi Θ-functions and thus admit an analytic treatment of the time asymptotics, which is given in the next section.

Solid handle bodies of genus $n \geq 2$ correspond to the choice of $2n$, $n \geq 2$, disks in the complex plane, as explained above. The covering group generated by the identifying transformations is a Schottky group; its limit set is a Cantor set lying in the interior of the disks (Akaza, 1964). Its Hausdorff dimension δ satisfies $0 < \delta < 2$, it is always greater than zero for $n \geq 2$. If δ is greater than one, then there exists a bound state with a localized wave field, and the convex hull of the limit set plays the same part with respect to the chaotic trajectories and localized wave fields as in the case of quasi-Fuchsian covering groups (Tomaschitz, 1992*a*).

Finally we discuss the deformation space, namely the space of nonisometric metrics of equal constant Gaussian curvature $-1/R^2$ on the 3-manifold. Two manifolds are exactly then isometric if their covering groups are conjugated (e.g., Bers, 1970; Krushkal *et al.*, 1986). Therefore on the Minkowski hyperboloid ($\Gamma = id$) there exists only one metric of Gaussian curvature $-1/R^2$. The deformation space of a solid torus can be parameterized by K, $|K| > 1$, because different moduli generate nonisometric covering groups. In Schottky groups, contrary to quasi-Fuchsian groups, there do not exist cycle relations among the generating transformations. Thus the

deformation space can be parameterized by $3(n-1)$ complex parameters, for there are n independent generators, each determined by its two fixed points and its modulus (Ford, 1951). By an overall conjugation of the group we can always move three of the fixed points to, say, 0, 1, ∞. That accounts for $6(n-1)$ real dimensions. Clearly F inherits always the Poincaré metric $d\sigma^2 = R^2 t^{-2}(|dz|^2 + dt^2)$ of H^3, but deformations of the polyhedral faces lead to globally nonisometric manifolds (Bers, 1970).

5. HOW IT WORKS IN THE SIMPLEST CASE: HOROSPHERICAL FLOWS, CLASSICAL AND QUANTUM CURRENTS, TOPOLOGICAL SCATTERING, AND SELF-INTERFERENCE

We study open RW cosmologies with solid tori as spacelike sections. We use the H^3 model of hyperbolic space and choose the fundamental polyhedron F of the 3-space as in Fig. 1a; the covering group is then Γ_K defined in Section 4. The pair (F, Γ_K) represents topologically a solid torus (cf. Fig. 1b).

Remark. The modulus K in Γ_K may be time dependent, varying on a path $K(\tau)$ in the deformation space (cf. Section 4) of the spacelike slices. It is in fact a typical feature of multiply connected RW geometries that time enters into the metric in two ways, via the expansion factor in (2.1) and globally via the choice of a path in the deformation space of the 3-space manifold (Tomaschitz, 1993*b*, 1994). The time dependence can lead to interesting effects, such as production/annihilation processes, and to angular anisotropy in the temperature of the microwave background (Tomaschitz, 1993*b*). In the following we keep K constant. This deformation space is conceptually close to Wheeler's superspace (Wheeler, 1973). However, we use it here to describe the variation of the metric in the large (the curvature stays constant, apart from a rescaling with the expansion factor), while Wheeler, as I understand it, uses it more on a microscopic level, trying to grasp topological and metrical quantum fluctuations of space-time.

In Tomaschitz (1993*a*) we defined a horospherical bundle of flow lines in H^3 as the collection of all geodesics issuing from one and the same point ξ on the boundary at infinity $\mathbb{C}$ of H^3. Clearly horospherical flows on the manifold $\mathbb{R}^{(+)} \times F$ are then obtained by projecting the flow lines into the polyhedron F by means of the canonical covering projection (see Figs. 2 and 3).

There are three types of qualitatively different trajectories in F, depending on whether two (Fig. 2), one (also Fig. 2), or none (Fig. 3a) of the endpoints of the covering trajectory lies in the limit set $\Lambda(\Gamma_K) = \{0, \infty\}$. In

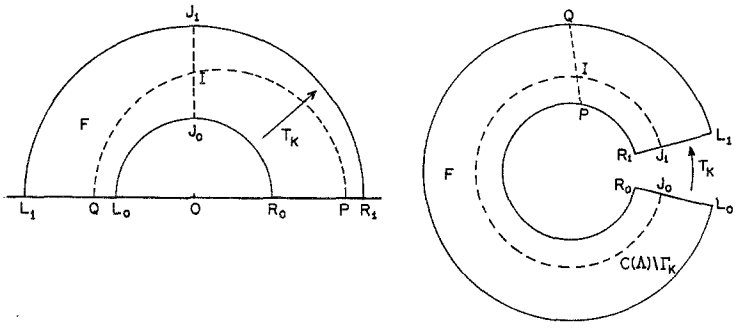

Fig. 1. (a) A section through the fundamental polyhedron F of a solid torus in the Poincaré half-space H^3. It is bounded by two concentric hemispheres of radius $|OR_0| = 1$ and $|OR_1| = |K|$ and an annulus of the same radii in the complex plane. The two hemispheres are the polyhedral faces that are identified by the transformation T_K. The third face in the complex plane, namely the annulus, represents the boundary of the torus at infinity of hyperbolic space, where the Poincaré metric gets singular. The hyperbolic volume of F is infinite. The arc QP represents a geodesic that connects two points at infinity. The term "boundary at infinity" is somewhat metaphoric; neither a particle nor a ray will reach this boundary within a finite time, there are no physical boundaries, and the 3-space is open and infinite. Likewise, if we speak about a solid torus we mean that in a purely topological sense, the product of a finite interval and an annulus. Fundamental polyhedra with face identification allow us to represent infinite spaces in a rather compact way, but at the expense of a singular metric induced onto them. If we identify the endpoints of J_0J_1 we obtain a geodesic loop. The existence of such loops is a typical physical manifestation of the topology. (b) We continuously deform the contour that represents a section through F in (a). The straight lines are bent to circular arcs, and vice versa. If we glue together the two ends of the figure by T_K, we get an annulus, a section through a solid torus (F, T_K). Indicated are also the two geodesics of (a).

the first case the projection is a closed loop $C(\Lambda)\backslash\Gamma_K$, the only one in the manifold. It is covered in H^3 by the convex hull $C(\Lambda)$ of the limit set, the straight line between $\xi = 0$ and $\xi = \infty$, orthogonal to the complex plane.

Remark. If the three-space is a manifold of higher connectivity ($n \geq 2$ in Section 4), with a Schottky or quasi-Fuchsian covering group, then the convex hull $C(\Lambda)$ is a three-dimensional domain, and likewise its projection $C(\Lambda)\backslash\Gamma$ in F, containing the chaotic trajectories and overwhelmingly fewer closed loops.

In the second case (Figs. 2 and 4b) the trajectories spiral out of (or into) $C(\Lambda)\backslash\Gamma_K$, their limit cycle. In the third case (Figs. 3a and 3b) the trajectory starts at the boundary and tends after some looping again toward the boundary. Which part of the trajectory is really run through by a geodesically moving particle depends on the time parametrization, determined

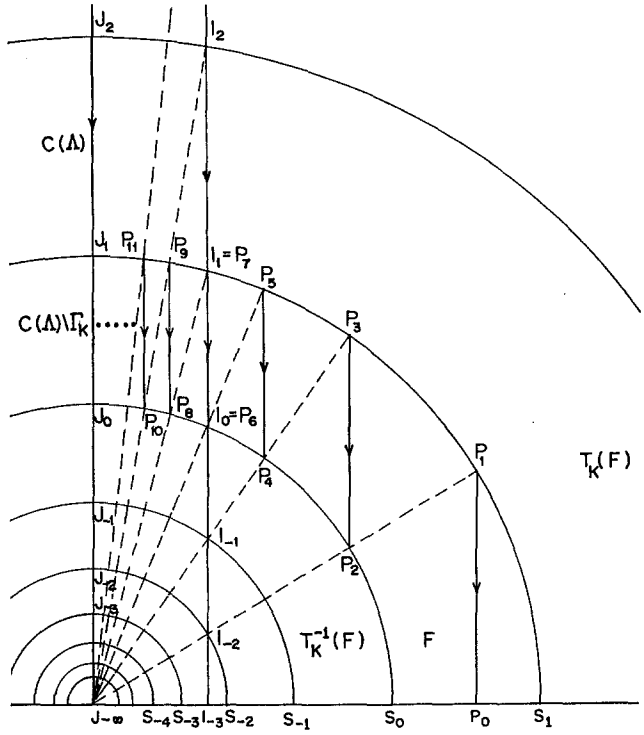

Fig. 2. If we apply the covering group Γ_K to F we get a tessellation of H^3 with concentric hemispherical shells, (S_n, S_{n+1}), $n \in \mathbb{Z}$. If we identify by T_K the endpoints of the geodesic arc J_0J_1, we obtain the limit cycle $C(\Lambda)\backslash\Gamma_K$. Its unique covering trajectory passing through J_n, $n = -\infty, \ldots, +\infty$, $\pi(J_nJ_{n+1}) = J_0J_1$, is the convex hull $C(\Lambda)$ of the limit set which consists of the points $J_{-\infty}$ and J_∞. The geodesic arcs P_nP_{n+1}, $n = 0, \ldots, \infty$, accumulate at J_0J_1. They constitute, if glued together, a trajectory in the manifold F that is spiraling out of $C(\Lambda)\backslash\Gamma_K$ (see also Fig. 4b). It is covered by the H^3 geodesic passing through I_n, $n = -3, \ldots, \infty$. The canonical covering projection $\pi(I_nI_{n+1}) = P_{2n+6}P_{2n+7}$ is indicated by the dashed rays. $K = 3/2$.

apart from the initial conditions by the expansion factor. For example, if $a(\tau) \sim \Lambda\tau$ for $\tau \to \infty$, the particle will come to rest well inside the manifold (Tomaschitz, 1991).

The most interesting case arises when the horospherical covering flow in H^3 emerges from a point in the limit set, from $\xi = 0$ or $\xi = \infty$. We may interchange these two fixed points by a conjugation, and so we choose $\xi = \infty$. Then the flow lines of the covering flow are the straight lines orthogonal to the boundary plane $\mathbb{C}$, and the horospheres of constant action are the Euclidean planes orthogonal to them; see Fig. 4. Moreover, for $\xi = \infty$ the H^3-Poisson kernel has a particularly simple form, $P = t/R$.

We use this expression for P in (2.10), construct the first series in (2.7) with the covering group Γ_K, and obtain for the classical density on $\mathbb{R}^{(+)} \times F$

$$\rho_c^{\Gamma}(t,\tau) \sim \frac{a^{-3}(\tau)t^2R^{-2}}{[1+2\alpha^2\beta^2B^2(\tau)]^{1/2}} \exp\left\{\frac{-\alpha^2}{1+2\alpha^2\beta^2B^2}\left[\log\frac{t}{R}+A(\tau)\right]^2\right\} \cdot \Theta(\mu_c,\lambda_c) \tag{5.1}$$

with

$$\Theta(\mu,\lambda) := \sum_{n=-\infty}^{+\infty} \exp(-\lambda n^2 + 2n\mu) \tag{5.2}$$

$$\mu_c(t,\tau) := \log|K| - \frac{\alpha^2\log|K|}{1+2\alpha^2\beta^2B^2(\tau)}\left[\log\frac{t}{R}+A(\tau)\right] \tag{5.3}$$

$$\lambda_c(\tau) = \frac{\alpha^2\log^2|K|}{1+2\alpha^2\beta^2B^2(\tau)} \tag{5.4}$$

Using the identity (Whittaker and Watson, 1984)

$$\Theta(\mu,\lambda) = \pi^{1/2}\lambda^{-1/2}\exp\left(\frac{\mu^2}{\lambda}\right)\Theta\left(\frac{-i\pi\mu}{\lambda},\frac{\pi^2}{\lambda}\right)$$
$$\mu,\lambda\in\mathbb{C}, \qquad \mathrm{Re}(\lambda)>0, \qquad -\pi/2<\arg\sqrt{\lambda}\le\pi/2 \tag{5.5}$$

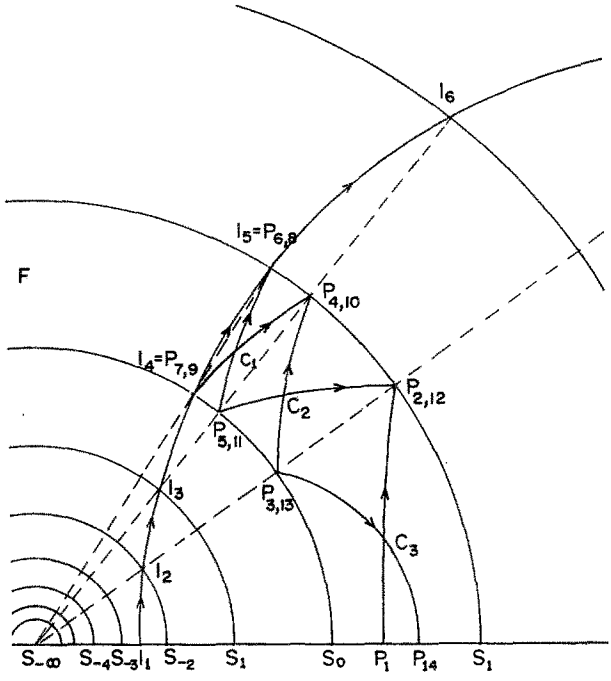

Fig. 3a

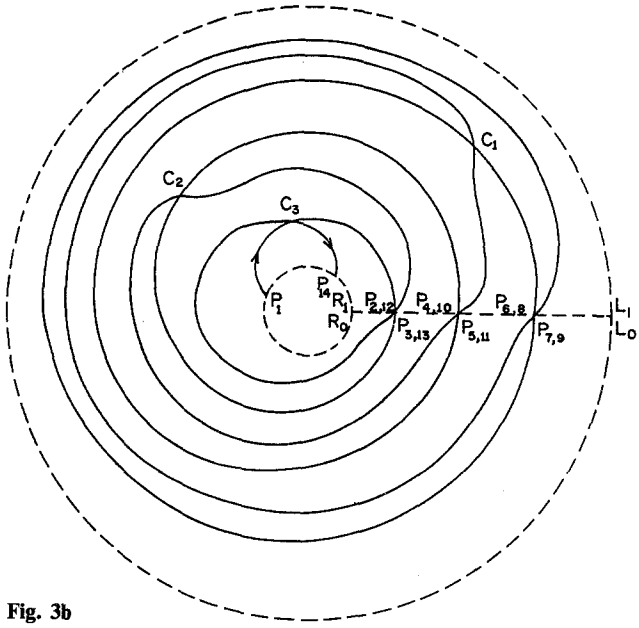

Fig. 3b

Fig. 3. (a) Covering trajectories may either be semicircles orthogonal to the boundary of H^3 (the complex plane) or Euclidean straight lines perpendicular to it. In this figure the covering trajectory has no endpoint in the limit set. Its projection $\pi(I_n I_{n+1}) = P_{2n-1}P_{2n}$, $n = 1, \ldots, 7$, starts at the boundary at infinity and tends again to the boundary after a finite number of loops. The circular arcs in F are glued together by the identification of the hemispheres S_0 and S_1 as depicted in Fig. 1a (via T_K). Initial and endpoints lying on the same dashed line are identified in this way; the same is the case in Fig. 2. The three trajectories in Figs. 2 and 3 exhaust all qualitatively different cases of geodesic motion on a solid torus. (b) The topology of the trajectory in (a). The fundamental polyhedron F in (a) is glued to a solid torus, as indicated in Figs. 1a and 1b. We indicate the points P_i of (a) that lie on the hemispheres S_0 and S_1, which are now glued together: $R_0 L_0$ is just S_0, and $R_1 L_1$ corresponds to S_1 (cf. Figs. 1a and 1b). The trajectory starts at P_1, arrives at P_2, P_2 and P_3 are identified, it moves on to P_4, P_4 and P_5 are identified, and so on. If $\mathrm{Im}(K) = 0$ (K is the modulus of T_K; cf. Section 4), the trajectory lies in a totally geodesic plane and is self-intersecting. In Fig. 2 and part (a) of this figure we assumed that this is the case. The arcs lie in a Euclidean plane orthogonal to the boundary of H^3. If K is complex, then the hemispheres S_0 and S_1 in Fig. 3a are rotated against each other before they are pointwise radially identified, and the geodesic arcs are no longer assembled in one plane.

we may write (5.1) as

$$\rho_c^{\Gamma}(t,\tau) \sim \frac{\sqrt{\pi}\, a^{-3}}{\alpha \log|K|} \exp\left[\frac{1+2\alpha^2\beta^2 B^2}{\alpha^2} - 2A(\tau)\right] \times \sum_{n=-\infty}^{+\infty} \exp -\left(\frac{n^2\pi^2}{\lambda_c} + \frac{2\pi i \mu_c n}{\lambda_c}\right) \tag{5.6}$$

From (5.3), (5.4), and (5.6) we have

$$\mu_c(|K|^m t, \tau) = \mu_c(t, \tau) - m\lambda_c(\tau), \qquad m \in \mathbb{Z} \tag{5.7}$$

and from that [actually, by definition (2.7)]

$$\rho_c^\Gamma(|K|^m t, \tau) = \rho_c^\Gamma(t, \tau) \tag{5.8}$$

First we investigate what happens if we confine a particle to a given trajectory on the manifold, in particular if we confine it to the limit cycle, by choosing the initial coordinates in the directions orthogonal to it with infinite precision. This amounts to replacing the ρ_c in (2.10) by

$$\rho_{z_0}(t, z, \tau) := \frac{\alpha R^2}{\sqrt{\pi}} \rho_c(t, \tau)\delta(z - z_0) \tag{5.9}$$

We use here complex notation, $(z, t) \in H^3$, and $\delta(y_1 + iy_2) := \delta(y_1)\delta(y_2)$; $\alpha R^2/\sqrt{\pi}$ is a normalization factor.

With $\delta(K^m z - z_0) = |K|^{-2m}\delta(z - K^{-m}z_0)$ we have on the manifold $\mathbb{R}^{(+)} \times F$

$$\rho_{z_0}^\Gamma(t, z, \tau) \sim \frac{\alpha}{\sqrt{\pi}} \frac{a^{-3}t^2}{[1 + 2\alpha^2\beta^2 B^2(\tau)]^{1/2}} \exp\left[\frac{-\alpha^2[\log(t/R) + A(\tau)]^2}{1 + 2\alpha^2\beta^2 B^2(\tau)}\right]$$
$$\times \sum_{n=-\infty}^{+\infty} \delta(z - K^{-n}z_0) \exp[-\lambda_c n^2 + 2n(\mu_c - \log|K|)] \tag{5.10}$$

with μ_c, λ_c as in (5.3), (5.4). If $z_0 = 0$, we can replace the series $\sum_{-\infty}^{+\infty}$ in (5.10) by $\delta(z)\Theta(\mu_c - \log|K|, \lambda_c)$, with Θ as in (5.2).

Applying (5.5) to (5.10), we obtain

$$\rho_{z_0=0}^\Gamma(t, z, \tau) \sim \frac{a^{-3}t^2\delta(z)}{\log|K|} \sum_{n=-\infty}^{+\infty} \exp -\left[\frac{n^2\pi^2}{\lambda_c} + \frac{2\pi i(\mu_c - \log|K|)n}{\lambda_c}\right] \tag{5.11}$$

If we integrate $\rho_{z_0}^\Gamma(t, z, \tau)$ over the manifold F by means of the hyperbolic volume element $dy_{H^3} = a^3 t^{-3}\, dy_1\, dy_2\, dt$, we have

$$\int_F \rho_{z_0}^\Gamma(t, z, \tau)\, dy_{H^3} = \int_{H^3} \rho_{z_0}(t, z, \tau)\, dy_{H^3} = 1 \tag{5.12}$$

Here we used the invariance of dy_H^3 under Γ and $\int_{H^3} = \sum_{\gamma \in \Gamma} \int_{\gamma(F)}$. The second integral in (5.12) is calculated in Tomaschitz (1993*a*). Equation (5.12) can also be directly verified for $z_0 = 0$, using term-by-term integration with (5.11).

Let us now discuss the foregoing a little. The $\rho_{z_0}^\Gamma$, $z_0 \neq 0$, in (5.10) is a probability density on the trajectory in Fig. 2 that spirals out of the limit cycle. Along this spiraling trajectory we can study the time asymptotics of

the energy and coordinate dispersion. Because the projection of the covering trajectory onto the spiraling trajectory is—contrary to the case $z_0 = 0$ treated below—bijective, the dispersion of $\rho^{\Gamma}_{z_0}$ on the spiraling trajectory in F is equivalent to the dispersion of ρ_c on the covering trajectory, namely the straight line through z_0 in H^3, and that has been studied in Tomaschitz (1993*a*) with respect to coordinates and energy.

For example, if the expansion is linear, $a(\tau) \sim \Lambda\tau$, $\tau \to \infty$, we have

$$\Delta x \sim c_1 a(\tau), \qquad v_P \sim c_2 \tau^{-1}, \qquad A \sim c_3, \qquad B \sim c_4 \tag{5.13}$$

v_P is the particle velocity, A, B are defined in (2.11), and the c_i are constants. Because $B \to \text{const} < \infty$, the packet stays peaked, and the dispersion of the coordinates is then merely due to the expansion of space, i.e., proportional to $a(\tau)$. Because $v_P \to 0$ the particle never reaches the boundary, and comes to rest at a finite point on the spiral in Fig. 4b.

If we compare that with the static case $a(\tau) = 1$,

$$\Delta x \sim c_1 \tau^2, \qquad v_P = c_2, \qquad A = c_3\tau, \qquad B = c_4\tau \tag{5.14}$$

we see that the width of the Gaussian goes to infinity in both directions of the time evolution. At $\tau = \infty$ the particle reaches the boundary at infinity of the torus; at $\tau = -\infty$ it rotates on the limit cycle, unlocalizable with constant density (compare also the case $z_0 = 0$ below).

Finally, backward in time, $a(\tau) \sim (\Lambda\tau)^{\lambda}$, $\lambda > 1$, $\tau \to 0$, we have

$$\Delta x \sim c_1 a(\tau), \qquad v_P \sim c_2, \qquad A \sim -c_3 \tau^{1-\lambda}, \qquad B \sim c_4 \tag{5.15}$$

which means that the density stays approximately a Gaussian that spirals for $\tau \to 0$ into the limit cycle. The dispersion Δx goes to zero because the length scale decreases. For further discussion on that we refer to Section 6.

Next we treat the case $z_0 = 0$ in (5.10), (5.11), where the particle is confined to the limit cycle $C(\Lambda)\backslash\Gamma_K$. If the width of the Gaussian in (5.10) is small compared to the length of the cycle,

$$\frac{\alpha^2}{1 + 2\alpha^2\beta^2 B^2} \gg \log^{-2}|K| \tag{5.16}$$

then $\lambda_c \gg 1$ in (5.4), and $\rho^{\Gamma}_{z_0=0}$ is essentially a Gaussian on $C(\Lambda)\backslash\Gamma_K$.

In the static case (5.14) we see that this Gaussian peak is washed out exponentially fast for $\tau \to \pm\infty$,

$$\rho^{\Gamma}_{z_0=0} = \delta(z)[\text{const} \cdot t^2 + O(\exp(-c\tau^2))]$$

[cf. (5.11)], which means that the probability measure is then proportional to dt/t, the hyperbolic line element on the limit cycle, i.e., we have a

uniform distribution on $C(\Lambda)\backslash\Gamma_K$ after an exponentially short time. In the other two cases (5.13) and (5.15), $\rho^{\Gamma}_{z_0=0}$ approaches a peaked limit distribution.

Before we discuss the density ρ^{Γ}_c in (5.1) and its quantum mechanical counterpart on the manifold $\mathbb{R}^{(+)} \times F$, we make some comments on the density (2.10). It is constant on a horosphere, $\log P(x, \eta) + c = 0$ (η, c fixed), and therefore not yet square-integrable with respect to the volume element of B^3. A further Gaussian average over the η variable has to be carried out, which makes it exponentially decaying along the horosphere toward the boundary of B^3 (Tomaschitz, 1993*a*). In (5.1) we preferred to periodize the density (2.10) as it stands, because it leads to a particularly transparent description of the wave motion, dispersion, and interference on the manifold $\mathbb{R}^{(+)} \times F$. We emphasize, however, that equations (5.1)–(5.8) and later the quantum version (5.18)–(5.22) can easily be generalized to η-averaged densities; equation (5.5) has then to be read as Poisson summation. As pointed out in Section 2, the involved series are rapidly convergent.

In Figs. 4 and 5 we depict the situation in the half-space model H^3. For the isometry $B^3 \leftrightarrow H^3$ and the boundary correspondence $\eta \leftrightarrow \xi$,

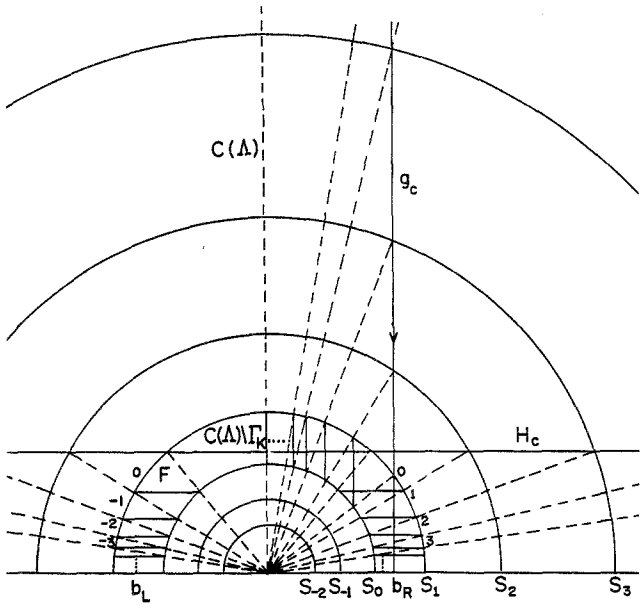

Fig. 4a

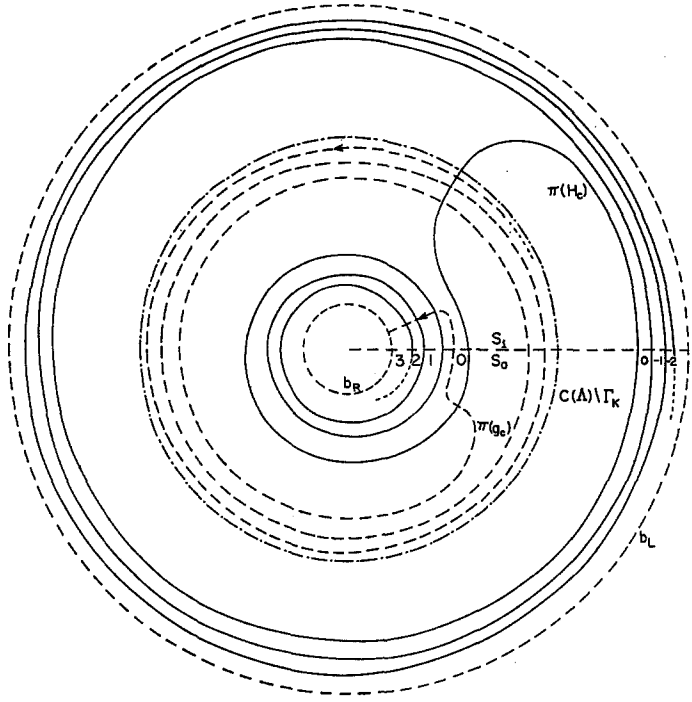

Fig. 4b

Fig. 4. (a) We depict here, as in Fig. 2, the tiling of H^3 by concentric hemispherical shells. There are two accumulation points of the tiles on the boundary of H^3, namely the common center of the hemispheres and the point at infinity, $\xi = \infty$, of the compactified complex plane, which are connected by the geodesic $C(\Lambda)$ (dashed). All geodesics that appear as Euclidean straight lines perpendicular to the complex plane originate in this point at infinity, e.g., $C(\Lambda)$ or g_c. They are parallel both in the Euclidean and hyperbolic sense. As in Fig. 2, we indicate the projection $\pi(g_c)$ of g_c into F via the dashed rays. The Euclidean plane H_c parallel to $\mathbb{C}$ is a horosphere, touching the boundary of H^3 at $\xi = \infty$. For another example of a horosphere see Fig. 5a. The projection mechanism of H_c into F is analogous to that of the geodesic g_c, and also indicated by dashed rays. The projection of H_c into F consists of annuli parallel to $\mathbb{C}$ that are orthogonally intersected by $\pi(g_c)$. The $\pi(H_c)$ is a surface of constant action for the flow lines spiraling out of the limit cycle. (b) The topology of the projected horosphere $\pi(H_c)$ of (a). As in Fig. 3b, we glue the polyhedron F in (a) to a torus. The identification of the polyhedral faces S_0 and S_1 in (a) also effects that the boundary circles of the annuli lying on S_0 and S_1 are glued together. We symbolize that by the dashed rays in (a) and carry it out here: $\pi(H_c)$ spirals toward infinity, partitioning the torus into shells, coded here by pairs $(n, -n)$, $n = 0, \ldots, \infty$. In the same way we code the shells in (a). The dashed spiral and the dot-dashed circle are just the $\pi(g_c)$ and the limit cycle $C(\Lambda)\backslash\Gamma_K$ of (a). The hyperbolic diameter of these shells approaches a finite value for $n \to \infty$.

$S_\infty \leftrightarrow \mathbb{C}$, see e.g., Beardon (1983). Because ρ_c in (2.10) is constant on every horosphere passing through ξ, it follows from (2.8) that ρ_c^Γ is constant on the canonical projections of the horospheres in F. If ξ is not in the limit set of Γ, then these projections are closed, in general self-intersecting surfaces of infinite area (Fig. 5b). If ξ lies in the limit set $\Lambda(\Gamma)$, then the projection of the H^3 horosphere is no longer closed. In Fig. 4a we depict the case $\xi = \infty$. The topology of the projected horosphere is indicated in Fig. 4b. It is spiraling toward infinity, partitioning the 3-space into toroidal shells which accumulate at infinity. In Fig. 4a every such shell is represented by the space between two annuli. Clearly the shells are connected through the identification of the two polyhedral faces by T_K.

The Euclidean distance of two annuli in Fig. 4a goes to zero if they approach $\mathbb{C}$; however, it is easy to see that their hyperbolic distance converges to a finite value, namely $Ra(\tau) \log|K|$, independent of the ordinate of the H^3 horosphere. Thus the shells close to the boundary have the same hyperbolic thickness. In the interior of the manifold the projected horosphere intersects orthogonally the limit cycle, whose hyperbolic length is again $Ra(\tau) \log|K|$. If we carry out the η averaging as discussed earlier, then ρ_c^Γ would be exponentially decaying along the spiraling horospherical projections toward the boundary at infinity.

ρ_c^Γ is invariant modulo a t-independent factor if we replace in μ_c the $A(\tau)$ by $A(\tau) + n \log|K|$, $n \in \mathbb{Z}$ [cf. (5.3), (5.6), and (5.7)]. The time evolution of ρ_c^Γ is—apart from a change of the width—periodic with respect to the

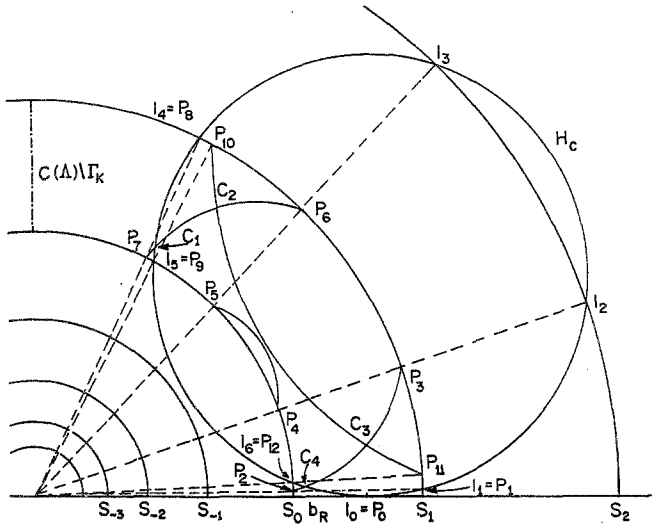

Fig. 5a

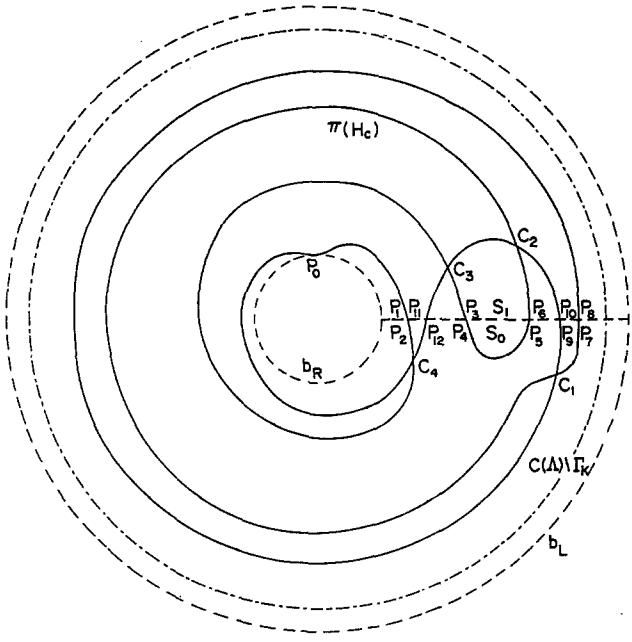

Fig. 5b

Fig. 5. (a) A horosphere is a Euclidean sphere tangent to the boundary at infinity (the horizon) of H^3. In this figure it originates from a finite point ξ $(=I_0)$ in $\mathbb{C}$, which is nevertheless at infinity of H^3. In Fig. 4a, H_c originates from $\xi=\infty$, and is so to say a sphere of infinite Euclidean radius. What really distinguishes the horospheres in Fig. 4a and here is not so much their Euclidean geometry, but rather that H_c in Fig. 4a originates from a point in the limit set of the covering group. The projection of H_c into F is coded by $\pi(I_nI_{n+1})=P_{2n}P_{2n+1}$, $\pi(I_6I_0)=P_{12}P_0$, $n=0,\ldots,5$, and consists of a finite number (because ξ lies outside the limit set) of overlapping spherical segments and caps. The projection and gluing procedure follows the usual pattern (cf. Fig. 3a) and is indicated by the dashed rays. $\pi(H_c)$ is a surface of constant action for the bundle of geodesics (not shown in the figure) issuing from ξ. It is also a wavefront of elementary waves excited at ξ [cf. (3.10)]. (b) The surfaces of constant action of horospherical flows can have quite an intricate topology. Depicted is a section through $\pi(H_c)$ in (a). The representation of the topology is the same as in Fig. 4b. The lettering is the same as in (a). The identification of the boundaries of the spherical segments and caps in the fundamental polyhedron of (a), symbolized there by the dashed rays, is carried out here. The points $P_1, P_{11}, P_3, P_6, P_{10}, P_8$ lying on S_1 are identified in pairs with $P_2, P_{12}, P_4, P_5, P_9, P_7$ on S_0, respectively. Remember and imagine, however, that $\pi(H_c)$ is two-dimensional, a closed self-intersecting surface of infinite hyperbolic area (because it touches the boundary at infinity at P_0), embedded in the three-dimensional torus; cf. the caption of Fig. 1a.

time intervals $\Delta\tau_n$ determined by

$$A(\tau + \Delta\tau_n) - A(\tau) = n \log|K| \tag{5.17}$$

Let us again assume that condition (5.16) holds true so that ρ_c^Γ in (5.1) is a Gaussian peaked along some horosphere. In the vicinity of the limit cycle this packet rotates in periods determined by (5.17). After n rotations its width has changed by a factor

$$\frac{a(\tau + \Delta\tau_n)}{a(\tau)} \frac{[1 + 2\alpha^2\beta^2 B^2(\tau + \Delta\tau_n)]^{1/2}}{[1 + 2\alpha^2\beta^2 B^2(\tau)]^{1/2}}$$

The first factor is due to the change of the length scale, the second gives the intrinsic broadening of the width.

Close to the boundary the packet crosses within a period $\Delta\tau_{i+1} - \Delta\tau_i$ the toroidal shells, and is afterward again concentrated on the same horosphere, its width having changed as above.

To treat finally the quantum case, we insert (3.8) into (3.2) and obtain

$$\psi \sim \frac{\varphi(\tau, s_0)(t/R)^{1 - is_0}}{(1 + i\alpha^2 f_{,ss})^{1/2}} \exp\left[-\frac{\alpha^2}{2} \frac{(\log(t/R) + f_{,s})^2}{1 + i\alpha^2 f_{,ss}} \right] \Theta(\mu_q, \lambda_q) \tag{5.18}$$

and for the density in (3.3) we get

$$\rho_q^\Gamma \sim \frac{a^{-3}}{(1 + \alpha^4 f_{,ss}^2)^{1/2}} \left(\frac{t}{R}\right)^2 \exp\left[\frac{-\alpha^2(\log(t/R) + f_{,s})^2}{1 + \alpha^4 f_{,ss}^2} \right] \cdot |\Theta(\mu_q, \lambda_q)|^2 \tag{5.19}$$

with Θ as in (5.2) and

$$\lambda_q(\tau) = \frac{\alpha^2}{2} \frac{\log^2|K|}{1 + \alpha^4 f_{,ss}^2} (1 - i\alpha^2 f_{,ss}) \tag{5.20}$$

and

$$\mu_q(t, \tau) = \frac{1}{2} \log|K| \left[\left(1 - \frac{\alpha^2(\log(t/R) + f_{,s})}{1 + \alpha^4 f_{,ss}^2} \right) - i \left(s_0 - \frac{\alpha^4 f_{,ss}(\log(t/R) + f_{,s})}{1 + \alpha^4 f_{,ss}^2} \right) \right] \tag{5.21}$$

Equations (5.7) and (5.8) hold true with the replacements (5.18)–(5.21).

With (5.5) we can write (5.18) as

$$\rho_q^\Gamma \sim \frac{2\pi a^{-3}}{\alpha^2 \log^2|K|} \exp\left(\frac{1 - s_0^2}{\alpha^2} - 2f_{,s} + 2s_0 f_{,ss} \right) \left| \Theta\left(\frac{-\pi\mu_q i}{\lambda_q}, \frac{\pi^2}{\lambda_q} \right) \right|^2 \tag{5.22}$$

If we replace the product $\Theta\bar{\Theta}$ in (5.19) by its diagonal part,

$$\operatorname{diag}(\Theta(\mu, \lambda)\Theta(\bar{\mu}, \bar{\lambda})) := \Theta(2\,\mathrm{Re}(\mu), 2\,\mathrm{Re}(\lambda))$$

[cf. (3.4), (3.13)], we obtain equation (5.1), provided

$$f_{,s} \sim A, \qquad 2\beta^2 B^2 \sim \alpha^2 f_{,ss}^2 \tag{5.23}$$

which is just the condition for the asymptotic equivalence of ρ_c [cf. (2.10)] and ρ_q [cf. (3.12)] in the covering space. Condition (5.23) holds true, for example, in the case of adiabatic expansion, and for the expansion factors in (5.13)–(5.15).

What is now the difference between (5.1) and (5.19)? What do the off-diagonal elements in $\Theta\bar{\Theta}$ effect? First, ψ^Γ is constant on the horospherical projections in Figs. 4a and 4b which are the wavefronts of ψ^Γ in $\mathbb{R}^{(+)} \times F$. Concerning the η averaging of (3.8), the same holds true as in the foregoing classical case: it effects the exponential decay of ψ^Γ along the horospherical projections. Analogously to equation (5.17), we have

$$f_{,s}(\tau + \Delta\tau_n) - f_{,s}(\tau) = n \log|K| \tag{5.24}$$

Let us now assume as in (5.16) that the width of the Gaussian in (5.19) is much smaller than the length of the limit cycle. As long as $\mathrm{Re}(\lambda_q) \gg 1$ [cf. Section 6) the $|\Theta|^2$ in (5.19) is negligible, and there is then no difference from the classical case. But when $f_{,ss}^2$ increases, so that the width gets comparable with $Ra(\tau) \log|K|$, then the fringes of the Gaussian in (5.18) start to overlap, and $\Theta\bar{\Theta}$ in (5.19) is no longer negligible, since $\mathrm{Re}(\lambda_q) \approx 1$. Because of the phases in the off-diagonal elements of $\Theta\bar{\Theta}$, new interference peaks appear in the distribution ρ_q^Γ. Also note that $\mathrm{Re}(\pi^2/\lambda_q)$ is independent of $f_{,ss}$, and ρ_q^Γ in (5.22) will not approach a uniform distribution on the limit cycle for $f_{,ss}^2 \to \infty$, contrary to the classical case $B^2 \to \infty$, discussed after (5.16).

6. CONCLUSION AND OUTLOOK

There is a natural length scale in universes of multiple spatial connectivity, provided by the hyperbolic diameter $d(C(\Lambda)\backslash\Gamma)$ of the convex hull of the limit set. In our example in Section 5 we have

$$d(C(\Lambda)\backslash\Gamma_K) = a(\tau) R \log|K| \tag{6.1}$$

which is clearly the length of the limit cycle. This cycle can be very small, depending on the choice of K. A wave packet dispersing in the vicinity of such a tiny loop can easily start to overlap and interfere with itself.

The mean wavelength of the packet in (5.18) is

$$\lambda_0 = \frac{2\pi}{s_0} Ra(\tau) \tag{6.2}$$

Its width is

$$\chi = Ra(\tau)\alpha^{-1}[(1 + \alpha^4 f_{,ss}^2)]^{1/2} \tag{6.3}$$

One may take $\alpha = \sqrt{s_0}$. If the curvature of 3-space is very small, then s_0 must be very large to obtain a moderate λ_0, and therefore the averaging takes place over a very narrow interval of wavelengths, $\Delta\lambda = s_0^{-1/2}\lambda_0$. Likewise we can assume $\alpha \log|K| \gg 1$ [cf. (6.5)].

In the case of linear expansion $a(\tau) \sim \Lambda\tau$, we have (Tomaschitz, 1992*c*)

$$f = \frac{mc^2}{\hbar}\tau - \frac{(1/4 + s_0^2)\hbar}{2mc^2\tau} + O(\tau^{-3}), \qquad f_{m=0} \sim s_0 \log \Lambda\tau \tag{6.4}$$

and with (6.1), (6.3),

$$\frac{\chi}{d} = \frac{1}{\alpha \log|K|}\left[1 + \frac{\alpha^4}{2}\frac{\hbar^2}{m^2c^4\tau^2} + O(\tau^{-4})\right], \qquad \left(\frac{\chi}{d}\right)_{m=0} \sim \frac{1}{\alpha \log|K|} \tag{6.5}$$

Thus the packet approaches a finite limit width on the scale of the expanding limit cycle (6.1); χ/d is here even decreasing. Whether a packet broadens or contracts depends on the choice of the phase of the wave function, but the d-scaled limit width is always finite under linear expansion. The f in (6.4) is determined only up to a τ-independent constant. We have chosen f so that (5.23) is satisfied with $\tau_0 = \infty$ in (2.11). If we choose the classical initial distribution at a finite τ_0, then we have to add a time-independent constant to f to achieve (5.23), and then the width broadens.

Even in the case $m = 0$, when the wave packet is moving with the speed of light, we have a finite limit width relative to the limit cycle. In particular there will be no self-interference, in striking contrast to the static case $a(\tau) = 1$, $f = (s_0^2 + R^2m^2c^2/\hbar^2)^{1/2}\Lambda\tau$, and $\chi/d \to \infty$.

Remark. We study here the dispersion orthogonal to the horospherical wavefronts; cf. the comments after (5.16). If we take a square-integrable wave packet, it will also disperse along the horospherical projections in F. However, this dispersion orthogonal to the direction of propagation will be certainly even smaller.

For the frequencies we have from (6.4)

$$\nu = \frac{mc^2}{2\pi\hbar} + \frac{(s_0^2 + 1/4)\hbar}{4\pi mc^2}\frac{1}{\tau^2} + O(\tau^{-4}), \qquad \nu_{m=0} \sim \frac{s_0}{2\pi\tau} \tag{6.6}$$

Finally we discuss the recurrence times of the densities on the limit cycle $C(\Lambda)\backslash\Gamma_K$ [cf. (5.24)]. We study this again in the context of packets that are infinitely extended orthogonal to their direction of propagation (cf. Section 5); in other words, we consider the rotations of the horospherical wavefronts. The generic situation, however, is that a square-integrable packet is driven away from the limit cycle and starts to spiral toward the boundary, like the classical trajectories. It stays confined to the limit cycle,

apart from dispersion, only if the covering packet in H^3 is centered at $C(\Lambda)$, the convex hull of the limit set.

Equation (5.24) with the $f_{m=0}$ in (6.4) is solved by $\Delta\tau \sim \tau(|K|-1)$. The package goes on rotating forever in linearly increasing periods, corresponding to the increase of the circumference of the limit cycle. If $m \neq 0$ and τ is sufficiently large, then equation (5.24) has no positive $\Delta\tau$ as solution; after a finite number of rotations the particle comes to rest.

In the early stage of the expansion, $a(\tau) \sim (\Lambda\tau)^{\lambda}$, $\tau \to 0$, $\lambda > 0$ [cf. (5.15)], with the phase f given in Tomaschitz (1993*a*) [cf. Eqs. (5.28), (5.36)], we have

$$\Delta\tau \sim \frac{1}{\Lambda}\frac{\log|K|}{s_0}(s_0^2+1-6\xi)^{1/2}(\Lambda\tau)^{\lambda} \tag{6.7}$$

and the packet is rotating independent of its mass with a frequency

$$\nu \sim \frac{\Lambda(s_0^2+1-6\xi)^{1/2}}{2\pi}(\Lambda\tau)^{-\lambda} \to \infty \tag{6.8}$$

and a group velocity $cs_0/(s_0^2+1-6\xi)^{1/2}$, $\xi \leq 1/6$.

We have for both massive and massless particles, if $\xi \neq 1/6$,

$$(\chi/d) \sim \text{const} \cdot \tau^{1-\lambda} \to \infty \tag{6.9}$$

and if $\xi = 1/6$,

$$\frac{\chi}{d} = \frac{1}{\alpha \log|K|}\left[1+\frac{\alpha^4}{2}\left(\frac{mc^2}{\hbar\Lambda}\right)^4\frac{(\Lambda\tau)^{2(1+\lambda)}}{(1+\lambda)^2 s_0^6}+O(\tau^{4(1+\lambda)})\right] \tag{6.10}$$

Thus, if the field is not conformally coupled, it disperses, and we have self-interference, as described in Section 5. In the conformally coupled case the packet has again an intrinsic finite limit width, so that it cannot overlap with itself on the limit cycle. Analogous considerations concerning dispersion hold true for the classical density (5.1), because of (5.23).

Clearly it would be interesting to compare the size of the limit cycle to atomic length scales. In order to do so we would have to know the point in the deformation space [the K in Eq. (6.1)] that determines the metric at present. Equations that determine the evolution of the metric in the deformation space are still lacking.

In a generic infinite 3-space of higher connectivity, the convex hull of the limit set is a three-dimensional finite domain. Its diameter defines then a length scale whose actual size is again determined by the choice of the metric in the deformation space of the 3-manifold. The chaoticity of the classical trajectories in the convex hull could be an explanation for the uniform distribution of galaxies.

Finally, topological self-interference leads to parity violation in the free Dirac equation on a multiply connected RW background (Tomaschitz, 1994). A P-reflected wave packet can cover the limit cycle and overlap with itself. This causes self-interference, its norm is not preserved, and accordingly P is not a unitary symmetry. The CPT symmetry is likewise broken.

ACKNOWLEDGMENTS

The author acknowledges the support of the European Communities through their Science Programme under grant B/SC1*-915078.

I also express my sincere thanks to Vinayak Wadke for the accurate drawings.

REFERENCES

Akaza, T. (1964). *Nagoya Mathematical Journal*, **24**, 43–64.

Beardon, A. (1983). *The Geometry of Discrete Groups*, Springer, Berlin.

Bers, L. (1970). *Annals of Mathematics*, **91**, 570–600.

Ford, L. (1951). *Automorphic Functions*, Chelsea, New York.

Krushkal, S. L., Apanasov, B. N., and Grusevskii, N. A. (1986). *Kleinian Groups and Uniformization in Examples and Problems*, American Mathematical Society, Providence, Rhode Island.

Landau, L. D., and Lifshitz, E. M. (1971). *The Classical Theory of Fields*, Pergamon, London.

Mandouvalos, N. (1988). *Proceedings of the London Mathematical Society*, **57**, 209–238.

Patterson, S. J. (1987). Lectures on measures on limit sets of Kleinian groups, in *Analytical and Geometrical Aspects of Hyperbolic Space*, D. B. A. Epstein, ed., Cambridge University Press, Cambridge, pp. 281–323.

Schrödinger, E. (1939). *Physica*, **6**, 899–912.

Schrödinger, E. (1956). *Expanding Universes*, Cambridge University Press, Cambridge.

Tomaschitz, R. (1991). *Journal of Mathematical Physics*, **32**, 2571–2579.

Tomaschitz, R. (1992*a*). *International Journal of Theoretical Physics*, **31**, 187–210.

Tomaschitz, R. (1992*b*). *Complex Systems* **6**, 137–161.

Tomaschitz, R. (1992*c*). Chaotic dynamics in general relativity, in *Chaotic Dynamics: Theory and Practice*, T. Bountis, ed., Plenum Press, New York, pp. 122–139.

Tomaschitz, R. (1993*a*). *Journal of Mathematical Physics*, **34**, 1022–1042.

Tomaschitz, R. (1993*b*). *Journal of Mathematical Physics*, **34**, 3133–3150.

Tomaschitz, R. (1994*a*). Classical and quantum chaos in extended RW cosmologies, in *Deterministic Chaos in General Relativity*, D. Hobill, ed., Plenum Press, New York, to appear.

Tomaschitz, R. (1994*b*). Cosmological CP violation, *Journal of Mathematical Physics*, **35**, to appear.

Wheeler, J. A. (1973). From relativity to mutability, in *The Physicist's Conception of Nature*, J. Mehra, ed., Reidel, Dordrecht, pp. 202–247.

Whittaker, E. T., and Watson, G. N. (1984). *A Course of Modern Analysis*, Cambridge University Press, Cambridge.